

Iron isotope effect on the superconducting transition temperature and the crystal structure of FeSe_{1-x}

R. Khasanov,^{1,*} M. Bendele,^{1,2} K. Conder,³ H. Keller,² E. Pomjakushina,³ and V. Pomjakushin⁴

¹Laboratory for Muon Spin Spectroscopy, Paul Scherrer Institute, CH-5232 Villigen PSI, Switzerland

²Physik-Institut der Universität Zürich, Winterthurerstrasse 190, CH-8057 Zürich, Switzerland

³Laboratory for Developments and Methods, Paul Scherrer Institute, CH-5232 Villigen PSI, Switzerland

⁴Laboratory for Neutron Scattering, ETH Zürich and PSI, CH-5232 Villigen PSI, Switzerland

The Fe isotope effect (Fe-IE) on the transition temperature T_c and the crystal structure was studied in the Fe chalcogenide superconductor FeSe_{1-x} by means of magnetization and neutron powder diffraction (NPD). The substitution of natural Fe (containing $\simeq 92\%$ of ^{56}Fe) by its lighter ^{54}Fe isotope leads to a shift of T_c of 0.22(5) K resulting in a Fe-IE exponent of $\alpha_{\text{Fe}} = 0.81(15)$. Analysis of NPD data suggests that more than a half of the observed T_c shift is caused by tiny structural modifications of $^{54}\text{FeSe}_{1-x}$, yielding an "intrinsic" shift of T_c (unrelated to structural changes) corresponding to a Fe-IE exponent of $\alpha_{\text{Fe}}^{\text{int}} = 0.33(16)$

PACS numbers: 74.70.Xa, 74.25.Jb, 61.05.F-

Historically, the isotope effect played a major role in elucidating the origin of the pairing interaction leading to the occurrence of superconductivity. The discovery of the isotope effect on the superconducting transition temperature T_c in Hg [1] in 1950 provided key experimental evidence for phonon-mediated pairing and supported the BCS theory of superconductivity in conventional low-temperature superconductors. The observation of unusually high T_c 's in the newly discovered Fe-based superconductors immediately raised the question regarding the pairing glue and initiated isotope effect studies. Currently, we are aware of two papers reporting, however, contradicting results. Liu *et al.* [2] showed that in $\text{SmFeAsO}_{0.85}\text{F}_{0.15}$ and $\text{Ba}_{0.6}\text{K}_{0.4}\text{Fe}_2\text{As}_2$ the Fe isotope effect (Fe-IE) exponent,

$$\alpha_{\text{Fe}} = -d \ln T_c / d \ln M_{\text{Fe}}, \quad (1)$$

reaches values of $\alpha_{\text{Fe}} \simeq 0.35$ (M_{Fe} is the Fe atomic mass), while Shirage *et al.* [3] found a negative Fe-IE exponent $\alpha_{\text{Fe}} \simeq -0.18$ in $\text{Ba}_{1-x}\text{K}_x\text{Fe}_2\text{As}_2$. Note that the only difference between the $\text{Ba}_{1-x}\text{K}_x\text{Fe}_2\text{As}_2$ samples studied in Refs. 2 and 3 was the preparation procedure (low-pressure synthesis in [2] *vs.* high-pressure synthesis in [3]), while the potassium doping ($x \simeq 0.4$) as well as the T_c 's for the samples containing natural Fe ($T_c \simeq 37.3$ K in [2] *vs.* $T_c \simeq 37.8$ K in [3]) were almost the same.

In this paper we report on studies of the Fe-IE on T_c and on the structural parameters (such as the lattice parameters a , b , and c , the lattice volume V , and the distance between the Se atom and Fe plane, Se height, h_{Se}) for another representative of the Fe-based high-temperature superconductors (HTS) FeSe_{1-x} . The "intrinsic" (unrelated to structural changes) shift of T_c corresponding to $\alpha_{\text{Fe}}^{\text{int}} = 0.33(16)$ was found to be in agreement with $\alpha_{\text{Fe}} \simeq 0.35$ obtained for $\text{SmFeAsO}_{0.85}\text{F}_{0.15}$ and $\text{Ba}_{0.6}\text{K}_{0.4}\text{Fe}_2\text{As}_2$ [2].

The $^{54}\text{FeSe}_{1-x}/^{56}\text{FeSe}_{1-x}$ samples (here after we denote natural Fe containing $\simeq 92\%$ of ^{56}Fe isotope as ^{56}Fe)

with the nominal composition $\text{FeSe}_{0.98}$ were prepared by a solid state reaction made in two steps. Pieces of Fe (natural Fe: 99.97% minimum purity, average atomic mass $M_{\text{Fe}} = 55.85$ g/mol, or ^{54}Fe : 99.99% purity, 99.84% isotope enriched, $M_{^{54}\text{Fe}} = 54.0$ g/mol) and Se (99.999% purity) were first sealed in double walled quartz ampules, heated up to 1075°C, annealed for 72 h at this temperature and 48 h at 420°C, and then cooled down to room temperature at a rate of 100°C/h. As a next step, the samples, taken out of the ampules, were powdered, pressed into pellets, sealed into new ampules and annealed first at 700°C for 48 h and then at 400°C for 36 h, followed by cooling to room temperature at a rate of 200°C/h. Due to the extreme sensitivity of FeSe_{1-x} to oxygen [4], all the intermediate steps (grinding and pelletizing) as well as the preparation of the samples for the neutron powder diffraction and magnetization experiments were performed in a glove box under He atmosphere.

The Fe-IE on the structural properties was studied in neutron powder diffraction (NPD) experiments by using the high-resolution powder diffractometer HRPT (Paul Scherrer Institute, Switzerland) [5]. The experiments were carried out at a wavelength $\lambda = 1.494$ Å. The $^{54}\text{FeSe}_{1-x}/^{56}\text{FeSe}_{1-x}$ samples, placed into vanadium containers, were mounted into a He-4 cryostat in order to reach temperatures between 5 and 250 K. High statistics data were taken at 250 and 5 K. Data at $10 \leq T \leq 240$ K were collected with intermediate statistics.

Figure 1 shows the NPD spectra taken at $T = 250$ K. The differences in peak intensities, clearly seen at the very beginning of the NPD spectra, are caused by the different values of the coherent neutron scattering length (b_{coh}) of natural Fe and that of the ^{54}Fe isotope. The refinement of the crystal structure was performed by using the FULLPROF program [6] with $b_{\text{coh}}^{\text{Fe}} = 9.45 \cdot 10^{-15}$ m, $b_{\text{coh}}^{^{54}\text{Fe}} = 4.2 \cdot 10^{-15}$ m, and $b_{\text{coh}}^{\text{Se}} = 7.97 \cdot 10^{-15}$ m [7]. The refined structural parameters at $T = 250$ K and 5 K

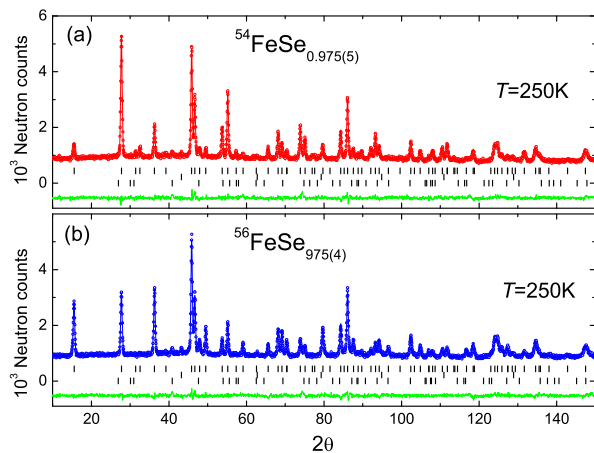


FIG. 1: (Color online) The Rietveld refinement pattern and difference plot of NPD data for $^{54}\text{FeSe}_{1-x}$ (panel a) $^{56}\text{FeSe}_{1-x}$ (panel b) at $T = 250$ K. The rows of ticks show the Bragg-peak positions for the main phase FeSe ($P4nmm$) and two impurity phases: Fe ($Im3m$) and hexagonal FeSe ($P6_3/mmc$). The main tetragonal phase corresponds to 0.975(5) and 0.975(4) Se occupancy for $^{54}\text{FeSe}_{1-x}$ and $^{56}\text{FeSe}_{1-x}$, respectively.

are summarized in Table 1. The amount of the impurity phases and the Se content ($1 - x$), determined for the data sets taken at $T = 250$ K, were kept fixed during the refinement of the NPD spectra taken at lower temperatures. The mass fractions of impurity phases, the hexagonal FeSe ($P6_3/mmc$) and Fe ($Im3m$), were found to be 0.50(10)%, 0.31(4)% and 1.13(18)%, 1.06(7)% for $^{54}\text{FeSe}_{1-x}$ and $^{56}\text{FeSe}_{1-x}$, respectively.

Figure 2 shows the temperature dependence of the lattice parameters a , b , and c , the lattice volume V , and the Se height h_{Se} of the $^{54}\text{FeSe}_{1-x}$ and $^{56}\text{FeSe}_{1-x}$ samples. Figure 2a implies that at $T \sim 100$ K, there is a transition from a tetragonal to an orthorhombic structure similar to that reported in [4, 8]. The Fe-IE on the structural transition temperature T_s could be estimated from the shift of the interception point of the linear fits to $a(T)$ and $b(T)$ in the vicinity of T_s , as denoted by the arrows in the inset of Fig. 2 a, which was found to be $\Delta T_s = 0.2(2.5)$ K (here after the Fe-IE shift of the quantity X is defined as $\Delta X = ^{54}X - ^{56}X$). This indicates that within the accuracy of the experiment there is no Fe-IE on T_s in FeSe_{1-x} .

Within the whole temperature range ($5 \text{ K} \leq T \leq 250 \text{ K}$) the lattice constants a and b are larger for $^{54}\text{FeSe}_{1-x}$ than that for $^{56}\text{FeSe}_{1-x}$ (see Fig. 2a). This is in contrast to the lattice parameter c , which over the whole temperature range is smaller for $^{54}\text{FeSe}_{1-x}$ than for $^{56}\text{FeSe}_{1-x}$ (Fig. 2b). The lattice volume remains, however, unchanged. Consequently, substitution of ^{56}Fe by ^{54}Fe leads to a small, but detectable, *enhancement* of the lattice along the crystallographic a and b directions and a *compression* of it along the c -axis. More important,

TABLE I: Structural parameters of $^{54}\text{FeSe}_{1-x}$ and $^{56}\text{FeSe}_{1-x}$ at $T = 250$ and 5 K. Space group $P4/nmm$ (no. 129), origin choice 2: Fe in (2b) position (1/4, 3/4, 1/2); Se in (2c) position (1/4, 1/4, z). Space group $Cmma$ (no. 67): Fe in (4b) position (1/4, 0, 1/2), Se in (4g) position (0, 3/4, z). The atomic displacement parameters (B) for Fe and Se were constrained to be the same. The Bragg R factor is given for the main phase; the other reliability factors are given for the whole refinement.

	$T = 250 \text{ K}$		$T = 5 \text{ K}$	
	$^{54}\text{FeSe}_{1-x}$	$^{56}\text{FeSe}_{1-x}$	$^{54}\text{FeSe}_{1-x}$	$^{56}\text{FeSe}_{1-x}$
Space group	$P4/nmm$		$Cmma$	
Se content	0.975(5)	0.975(4)	fixed to 0.975	
$a(\text{\AA})$	3.77036(3)	3.76988(5)	5.33523(10)	5.33426(10)
$b(\text{\AA})$			5.30984(10)	5.30933(10)
$c(\text{\AA})$	5.51619(9)	5.51637(9)	5.48683(9)	5.48787(9)
Volume (\AA^3)	156.883(3)	156.797(3)	155.438(5)	155.424(5)
$z\text{-Se}$	0.2319(2)	0.2326(0.3)	0.2321(2)	0.2322(3)
$B(\text{\AA}^2)$	1.02(2)	0.93(2)	0.44(2)	0.36(2)
R_{Bragg}	3.11	2.93	4.13	3.63
R_{wp}	3.93	3.72	5.16	4.62
R_{exp}	3.13	3.05	4.73	4.03
χ^2	1.58	1.49	1.19	1.32

such structural modifications should affect the shape of the Fe_4Se pyramid, which has a strong influence on T_c in Fe-based HTS [9–11]. This is obviously the case. Fig. 2 c reveals that below 100 K the Se atom is located closer to the Fe plane in $^{54}\text{FeSe}_{1-x}$ than in $^{56}\text{FeSe}_{1-x}$. The corresponding change of the Fe_4Se pyramid is shown schematically in the inset of Fig. 2 c.

The Fe-IE on T_c was studied by means of magnetization experiments. Measurements were performed by using a SQUID magnetometer (Quantum Design MPMS-7) in a field of $\mu_0 H = 0.1$ mT for temperatures ranging from 2 to 20 K. It is important to note that T_c of FeSe_{1-x} was found to be very sensitive to the Se content. McQueen *et al.* [12] showed that a decrease of the Se content by $\simeq 1\%$ (from $1 - x \simeq 0.99$ to 0.98) leads to a shift of T_c of 2 to 2.5 K. In order to ensure the "intrinsic" nature of the Fe-IE it is important to perform a *statistical* study: *i.e.* to investigate series of $^{54}\text{FeSe}_{1-x}/^{56}\text{FeSe}_{1-x}$ samples synthesized exactly the same way (the same thermal history, the same amount of Se in the initial composition). The magnetization experiments presented below were conducted for six $^{54}\text{FeSe}_{1-x}$ and seven $^{56}\text{FeSe}_{1-x}$ samples, respectively.

The inset in Fig. 3 shows an example of zero-field cooled (ZFC) magnetization curves for a pair of $^{54}\text{FeSe}_{1-x}/^{56}\text{FeSe}_{1-x}$ samples (M_{norm} was obtained after subtracting the small paramagnetic offset M_{magn} measured at $T > T_c$ and further normalization of the

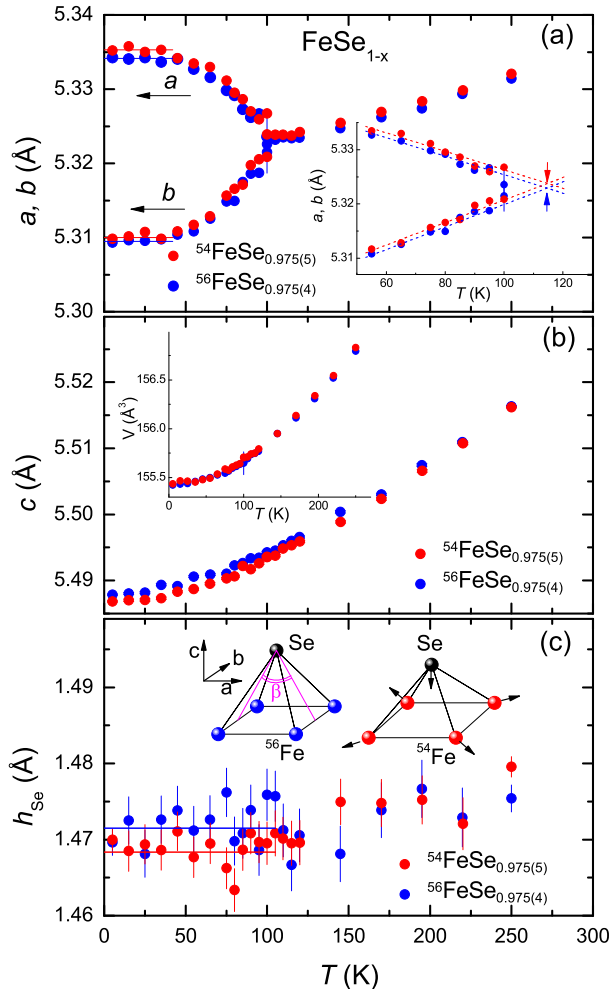


FIG. 2: (Color online) The temperature dependence of the lattice constants a and b (panel a, in the tetragonal phase a is multiplied by $\sqrt{2}$), lattice constant c (panel b), and the distance between the Se atom and Fe plane h_{Se} (panel c) for $^{54}\text{FeSe}_{0.975(5)}$ and $^{56}\text{FeSe}_{0.975(4)}$ samples. The inset in panel a shows the extended part of $a(T)$ and $b(T)$ in the vicinity of the structural transition temperature T_s together with the linear fits. The inset in panel b represents the temperature dependence of the lattice volume V . The inset in panel c shows schematically the modification of the Fe_4Se pyramid caused by ^{56}Fe to ^{54}Fe isotope substitution. The arrows show the direction of atom displacements (see text for details).

obtained curve to the value at $T = 2$ K, see Fig. 1 in Ref. 4 for details). The magnetization curve for $^{54}\text{FeSe}_{1-x}$ is shifted almost parallel to higher temperature, implying that T_c of $^{54}\text{FeSe}_{1-x}$ is higher than that of $^{56}\text{FeSe}_{1-x}$. The resulting transition temperatures determined from the intercept of the linearly extrapolated $M_{\text{norm}}(T)$ curves with the $M = 0$ line for all samples investigated are summarized in Fig. 3. The T_c 's for both sets of $^{54}\text{FeSe}_{1-x}/^{56}\text{FeSe}_{1-x}$ samples fall into two distinct regions: $8.39 \leq ^{54}T_c \leq 8.48$ K and $8.15 \leq ^{56}T_c \leq 8.31$ K, respectively. The corresponding mean values are: $^{54}\bar{T}_c = 8.43(3)$ K and $^{56}\bar{T}_c = 8.21(4)$ K.

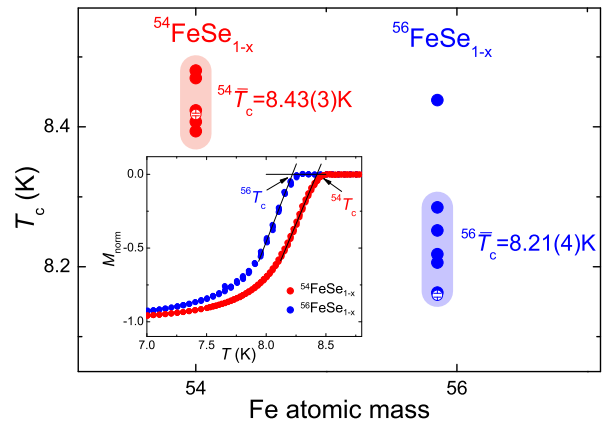


FIG. 3: (Color online) The superconducting transition temperature T_c as function of Fe atomic mass for $^{54}\text{FeSe}_{1-x}/^{56}\text{FeSe}_{1-x}$ samples studied in the present work. The open symbols correspond to the samples studied by NPD experiments. The T_c 's fall into the regions marked by the colored stripes with the corresponding mean values $^{54}\bar{T}_c = 8.43(3)$ K and $^{56}\bar{T}_c = 8.21(4)$ K. The inset shows the normalized ZFC magnetization curves $M_{\text{norm}}(T)$ for one pair of $^{54}\text{FeSe}_{1-x}$ and $^{56}\text{FeSe}_{1-x}$ samples. The transition temperature T_c is determined as the intersection of the linearly extrapolated $M_{\text{norm}}(T)$ curve in the vicinity of T_c with the $M = 0$ line.

Note that one out of the seven $^{56}\text{FeSe}_{1-x}$ samples had $T_c \simeq 8.44$ K which is by more than 5 standard deviations above the average calculated for the rest of the six samples. We have no explanation for this discrepancy, but decided to show this point for completeness of the data collected.

The Fe-IE exponent defined by means of Eq. (1) was found to be $\alpha_{\text{Fe}} = 0.81(15)$. Two important points need to be considered: i) The *positive* sign of the Fe-IE exponent α_{Fe} is similar to that observed in phonon mediated superconductors, such as elemental metals [1] and MgB_2 [13] as well as in cuprate HTS [14, 15] where the pairing mechanism is still under debate. Bearing in mind that a positive Fe-IE exponent was also observed in $\text{SmFeAsO}_{0.85}\text{F}_{0.15}$ and $\text{Ba}_{0.6}\text{K}_{0.4}\text{Fe}_2\text{As}_2$ [2], we may conclude that at least for three compounds representing different families of Fe-based HTS (1111, 122, and 11) the sign of the Fe-IE on T_c is conventional. This suggests that the lattice degrees of freedom play an essential role in the occurrence of superconductivity in the Fe-based HTS. ii) The Fe-IE exponent $\alpha_{\text{Fe}} = 0.81(15)$ is larger than the universal BCS value $\alpha^{\text{BCS}} = 0.5$ as well as more than twice as large as $\alpha_{\text{Fe}} \simeq 0.35$ reported for $\text{SmFeAsO}_{0.85}\text{F}_{0.15}$ and $\text{Ba}_{0.6}\text{K}_{0.4}\text{Fe}_2\text{As}_2$ [2]. Note that a high value of the oxygen isotope exponent ($\alpha_{\text{O}} \gtrsim 1$) was also observed in underdoped cuprate HTS [15] and was explained to be a consequence of the polaronic nature of the supercarriers in that class of materials [16]. However Bussmann-Holder *et al.* [17] recently showed that polaronic effects in Fe-based HTS are expected to

be much weaker than in underdoped cuprate HTS and that $\alpha_{\text{Fe}} \lesssim 0.5$.

Therefore we assume that a substantial part of the Fe-IE exponent $\alpha_{\text{Fe}} = 0.81(15)$ results from tiny structural changes, as observed in the NPD experiments presented above. Indeed, in FeSe_{1-x} the decrease of the Se height caused by compression of the Fe_4Se pyramid leads to an increase of T_c by $\Delta T_c^{h_{\text{Se}}}/(\Delta h_{\text{Se}}/h_{\text{Se}}) \simeq 3.4 \text{ K}/\%$ [11, 18]. In contrast, the increase of the Se(Te)-Fe-Se(Te) angle in the $\text{FeSe}_{1-y}\text{Te}_y$ family (angle β in our notation [19], see the inset of Fig. 2c) results for $y \lesssim 0.5$ in a decrease of T_c by $\Delta T_c^\beta/(\Delta\beta/\beta) \simeq 2.9 \text{ K}/\%$ [10]. Based on the structural data presented in Fig. 2 one obtains $\Delta h_{\text{Se}}/h_{\text{Se}} = 0.22(8)\%$ and $\Delta\beta/\beta = -0.13(4)\%$, leading to $\Delta T_c^{h_{\text{Se}}} = 0.7(3) \text{ K}$ and $\Delta T_c^\beta = -0.4(2) \text{ K}$ (in this estimate the values of the lattice constants a and b , and h_{Se} were averaged over the temperature regions denoted as solid lines in Figs. 2a and c). Bearing in mind that almost all Fe-based HTS are as sensitive to structural changes as FeSe_{1-x} (see, *e.g.*, [9–11]) we conclude that the shift of T_c caused by tiny modifications of the crystal structure may contribute substantially to the total Fe-IE exponent. More important, for some sorts of distortions the "structural effects" could result in a relatively high value of α_{Fe} (as $\alpha_{\text{Fe}} \simeq 0.8$ observed here) or may even cause a change of sign in α_{Fe} .

The above discussion does not allow, however, to estimate the absolute value of the "structural" correction to the total Fe-IE exponent. The main reason is the relatively large error of h_{Se} which mostly contributes to the uncertainties in $\Delta T_c^{h_{\text{Se}}} = 0.7(3) \text{ K}$ and $\Delta T_c^\beta = -0.4(2) \text{ K}$. On the other hand, the lattice constants a , b , and c could be determined with much better precision. We used, therefore, the empirical T_c vs. a dependence for $\text{FeSe}_{1-y}\text{Te}_y$ from [10] which for $y \lesssim 0.5$ gives $\Delta T_c^a/(\Delta a/a) \simeq 6.6 \text{ K}/\%$. For $(\Delta a + \Delta b)/(a + b) = 0.0195(14)\%$ the "structural" and the "intrinsic" (unrelated to structural changes) Fe-IE exponents were found to be $\alpha_{\text{Fe}}^{\text{str}} = 0.48(16)$ and $\alpha_{\text{Fe}}^{\text{intr}} = 0.33(16)$, respectively. Here the values of the lattice constants a and b were averaged over the temperature regions shown in Fig. 2a.

To summarize, the $^{54}\text{Fe}/^{56}\text{Fe}$ isotope effects on the superconducting transition temperature and the crystal structure were studied in the iron chalcogenide superconductor FeSe_{1-x} . The following results were obtained: (i) The substitution of the natural Fe ($M_{\text{Fe}} = 55.85 \text{ g/mol}$) by the ^{54}Fe isotope ($M_{^{54}\text{Fe}} = 54.0 \text{ g/mol}$) leads to an enhancement of the lattice constants a and b and shrinkage of the lattice constant c . These modifications do not affect the lattice volume. (ii) The tetragonal to orthorhombic structural transition temperature ($T_s \sim 100 \text{ K}$) is the same for both $^{54}\text{FeSe}_{1-x}$ and $^{56}\text{FeSe}_{1-x}$ within the accuracy of the experiment. (iii) For temperatures below 100 K the distance between the Se atom and Fe plane (Se height) is smaller for the samples with ^{54}Fe . This, together with the results of point i), suggest that ^{56}Fe

to ^{54}Fe isotope substitution leads to a compression of the Fe_4Se pyramid along the crystallographic c -axis and an enhancement along the a - and b -directions. (vi) The average superconducting transition temperature is $\simeq 0.22 \text{ K}$ higher for the $^{54}\text{FeSe}_{1-x}$ samples than that for the $^{56}\text{FeSe}_{1-x}$ ones resulting in a Fe-IE exponent of $\alpha_{\text{Fe}} = 0.81(15)$. (v) The structural changes caused by the ^{56}Fe to ^{54}Fe isotope substitution results in a shift of T_c of $\Delta T_c^{\text{str}} \simeq 0.13 \text{ K}$, which corresponds to $\alpha_{\text{Fe}}^{\text{str}} \simeq 0.48$. The "intrinsic" (unrelated to structural changes) Fe-IE exponent $\alpha_{\text{Fe}}^{\text{intr}} = 0.33(16)$ is in agreement with $\alpha_{\text{Fe}} \simeq 0.35$ obtained for $\text{SmFeAsO}_{0.85}\text{F}_{0.15}$ and $\text{Ba}_{0.6}\text{K}_{0.4}\text{Fe}_2\text{As}_2$ [2].

To conclude, the tiny changes of the crystallographic parameters caused by isotope substitution may contribute substantially to the total Fe-IE exponent. Reliable studies of the isotope effect in the newly discovered Fe-based HTS require also detailed and careful investigations of the crystal structure. The observation of a pronounced iron isotope effect on T_c with a positive value of the Fe-IE exponent demonstrates that the lattice degrees of freedom are essential for superconductivity in the Fe-based HTS.

This work was partly performed at SINQ (Paul Scherrer Institute, Switzerland). The work of MB was supported by the Swiss National Science Foundation. The work of EP was supported by the NCCR program MaNEP.

* Corresponding author: rustem.khasanov@psi.ch

- [1] E. Maxwell, Phys. Rev. **78**, 477 (1950); C.A. Reynolds *et al.*, Phys. Rev. **78**, 487 (1950).
- [2] R.H. Liu *et al.*, Nature **459**, 64 (2009).
- [3] P.M. Shirage *et al.*, Phys. Rev. Lett. **103**, 257003 (2009).
- [4] E. Pomjakushina *et al.*, Phys. Rev. B **80**, 024517 (2009).
- [5] P. Fischer, Physica B **276-278**, 146 (2000).
- [6] J. Rodríguez-Carvajal, Physica B **192**, 55 (1993).
- [7] <http://www.ncnr.nist.gov/resources/n-lengths>
- [8] S. Margadonna *et al.*, Chem. Commun. (Cambridge) **5607** (2008).
- [9] J. Zhao *et al.*, Nature Materials **7**, 953 (2008).
- [10] K. Horigane *et al.*, J. Phys. Soc. Jpn. **78**, 07418 (2009).
- [11] Y. Mizuguchi *et al.*, arXiv:1001.1801.
- [12] T.M. McQueen *et al.*, Phys. Rev. B **79**, 014522 (2009).
- [13] S.L. Budko *et al.*, Phys. Rev. Lett. **86**, 1877 (2001); D.G. Hinks, H. Claus, and J.D. Jorgensen, Nature **411**, 457 (2001).
- [14] B. Batlogg *et al.*, Phys. Rev. Lett. **59**, 912 (1987); J.P. Franck *et al.*, Phys. Rev. B **44**, 5318 (1991).
- [15] R. Khasanov *et al.*, Phys. Rev. Lett. **101**, 077001 (2008).
- [16] A. Bussmann-Holder and H. Keller, Eur. Phys. J. B **44**, 487 (2005).
- [17] A. Bussmann-Holder *et al.*, arXiv:0906.2283; A. Bussmann-Holder *et al.*, to appear in J. Supercond. Nov. Magn. (DOI:10.1007/s10948-009-0586-2).
- [18] S. Margadonna *et al.*, Phys. Rev. B **80**, 064506 (2009).
- [19] In the orthorhombic phase there are two angles β_1 and β_2 which are different by $\simeq 0.3^\circ$ at $T = 5 \text{ K}$.